Mechanism of 150-Cavity Formation in Influenza Neuraminidase

Rommie E. Amaro[1,] Robert V. Swift[1], Lane Votapka[1], Wilfred Li[2], Ross C. Walker[3], and Robin Bush[4]

[1] Department of Pharmaceutical Sciences, Computer Science, and Chemistry, University of California, Irvine, Irvine, CA, USA. [2] National Biomedical Computation Resource, University of California, San Diego, La Jolla, CA, USA. [3] Department of Chemistry and Biochemistry & San Diego Supercomputer Center, University of California, San Diego, La Jolla, CA, USA. [4] Department of Ecology and Evolution, University of California, Irvine, Irvine, CA, USA. Correspondence should be addressed to R.E.A. (ramaro@uci.edu)

Supplementary Figures:

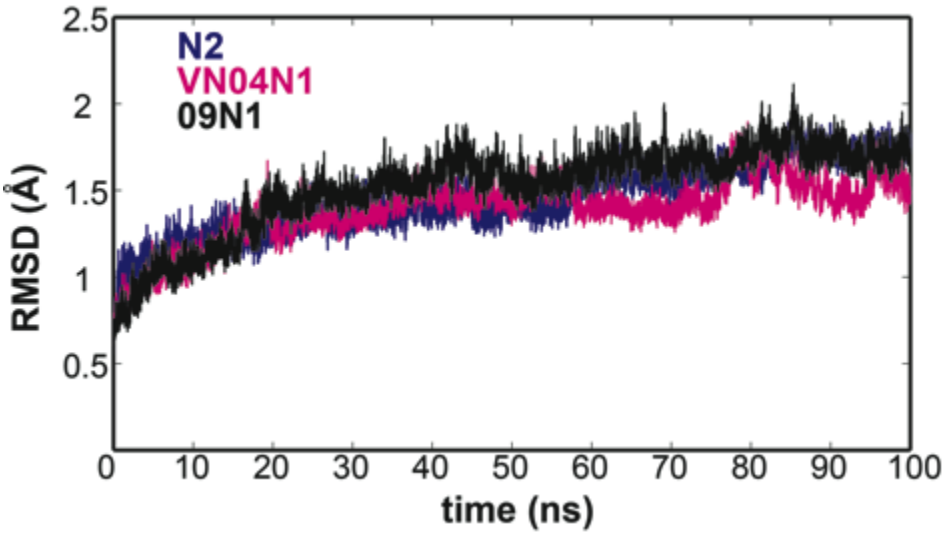

Supplementary Figure S1: The time series for the RMSD over alpha-carbon atoms for tetramer systems is shown for each 100 ns simulation (for reference, N2 is shown in blue, VN04N1 in pink, and 09N1 in black). The plot indicates stability of the simulated systems.

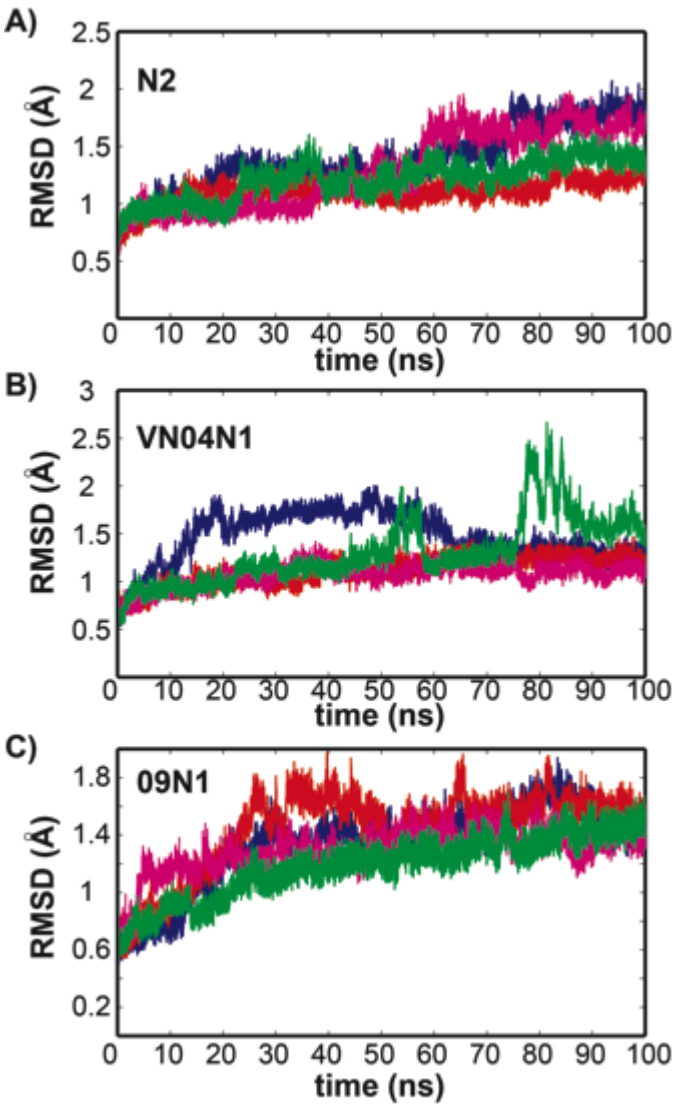

Supplementary Figure S2: The time series for the per monomer RMSD, as computed over the alpha-carbons, is shown for the N2, VN04N1, and 09N1 systems. For all systems, chain A is shown in blue, chain B in red, chain C in fuschia, and chain D in green.

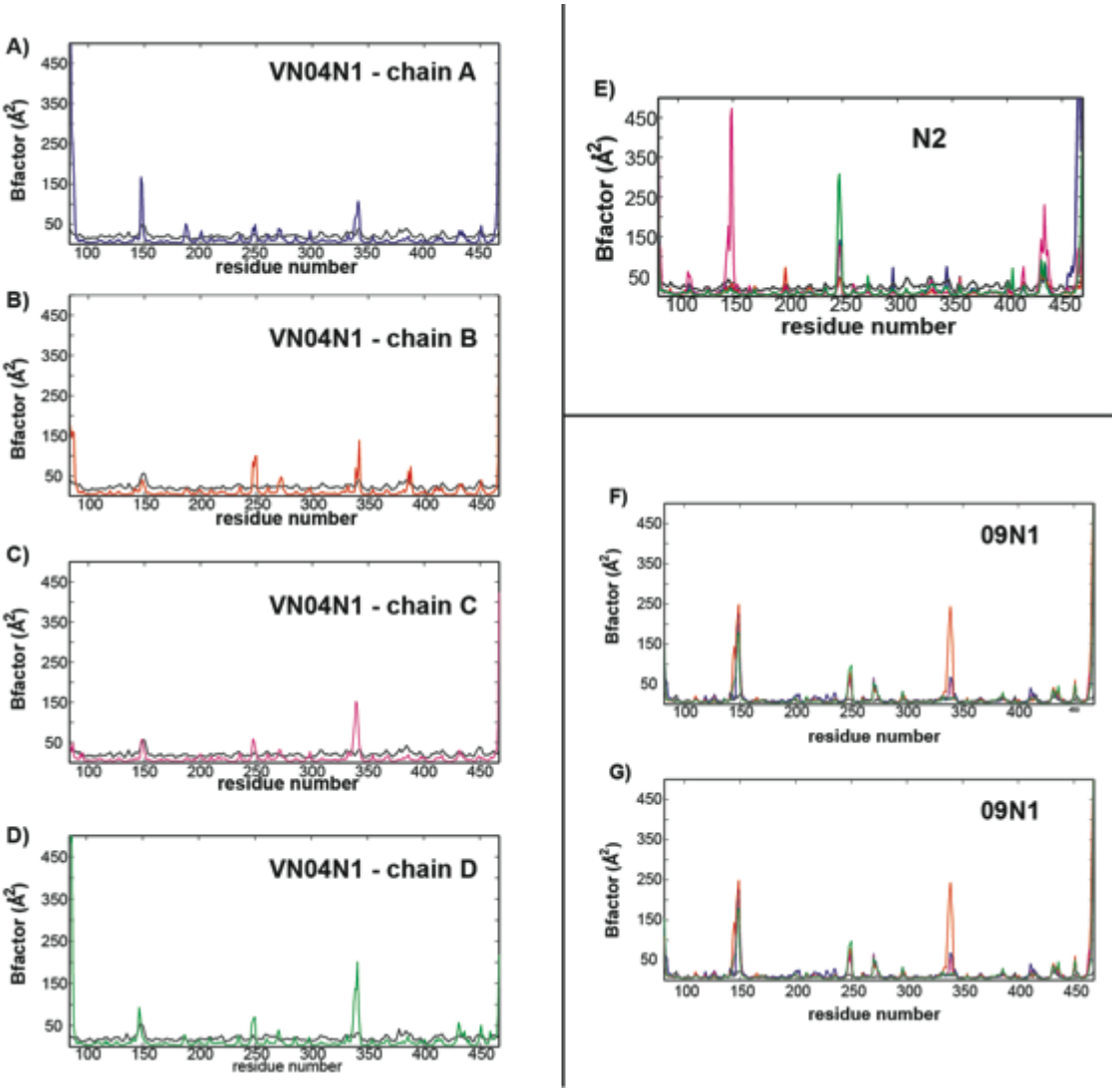

Supplementary Figure S3: Experimental and simulation-derived B-factors. Crystal B-factors shown in black throughout. MD-derived B-factors shown in blue, orange, fuchsia, and green for tetramer chains A, B, C, D, respectively. A-D) VN04N1 PDB 2HTY is a tetramer; B-factors for each chain are compared individually. E) N2 PDB 1NN2 has one chain; all 4 MD chains are shown, F-G) 09N1 PDB 3NSS has 2 chains; all 4 MD monomers are shown against chain A (in F) and chain B (in G).

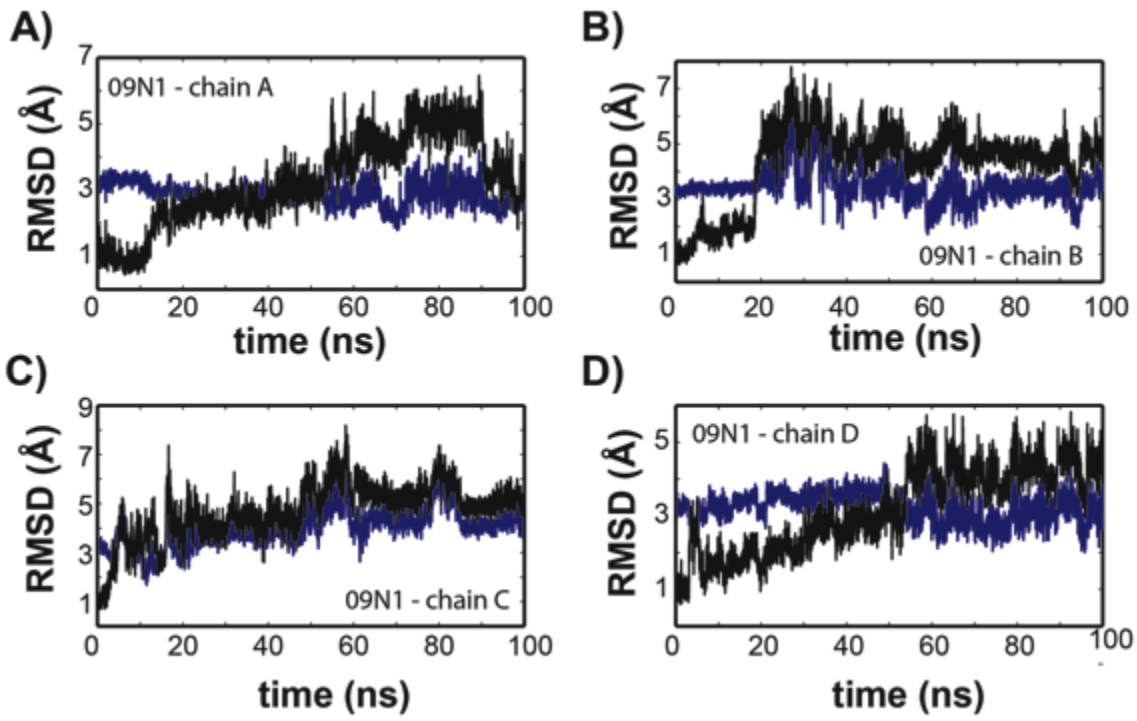

Supplementary Figure S4: The structural deviations in the 150-loop (residues 146-152) are shown for the 09N1 system. 150-loop RMSD from the open- (shown in blue) and closed- (shown in black) 150-loop crystal structures (2HTY and 2HU4, respectively) indicate structural deviations from the experimentally resolved data. Locations where the two lines cross over indicate a loop "switching event" (from open to closed, or closed to open).

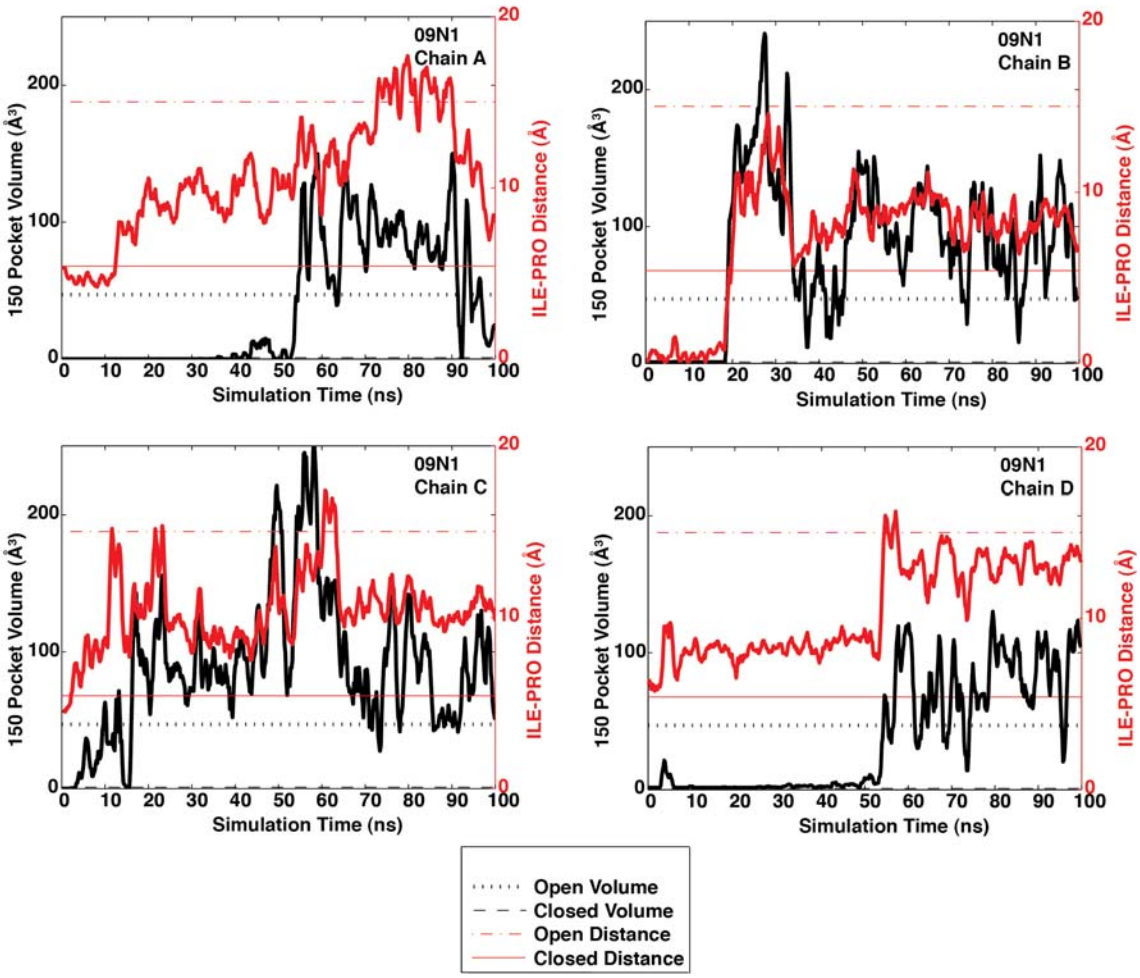

Supplementary Figure S5: Time series analysis of 150-cavity volume and width for 09N1 system. The distance between alpha carbon of residue 431 (Pro431 in 09N1) and the closest sidechain carbon of residue 149 (Ile149 in 09N1) is computed and shown in red and the right-side y-axis. On the left side y-axis, the volume of the 150-cavity is computed over the course of simulation. Each plot represents a chain of the neuraminidase tetramer (A-D).

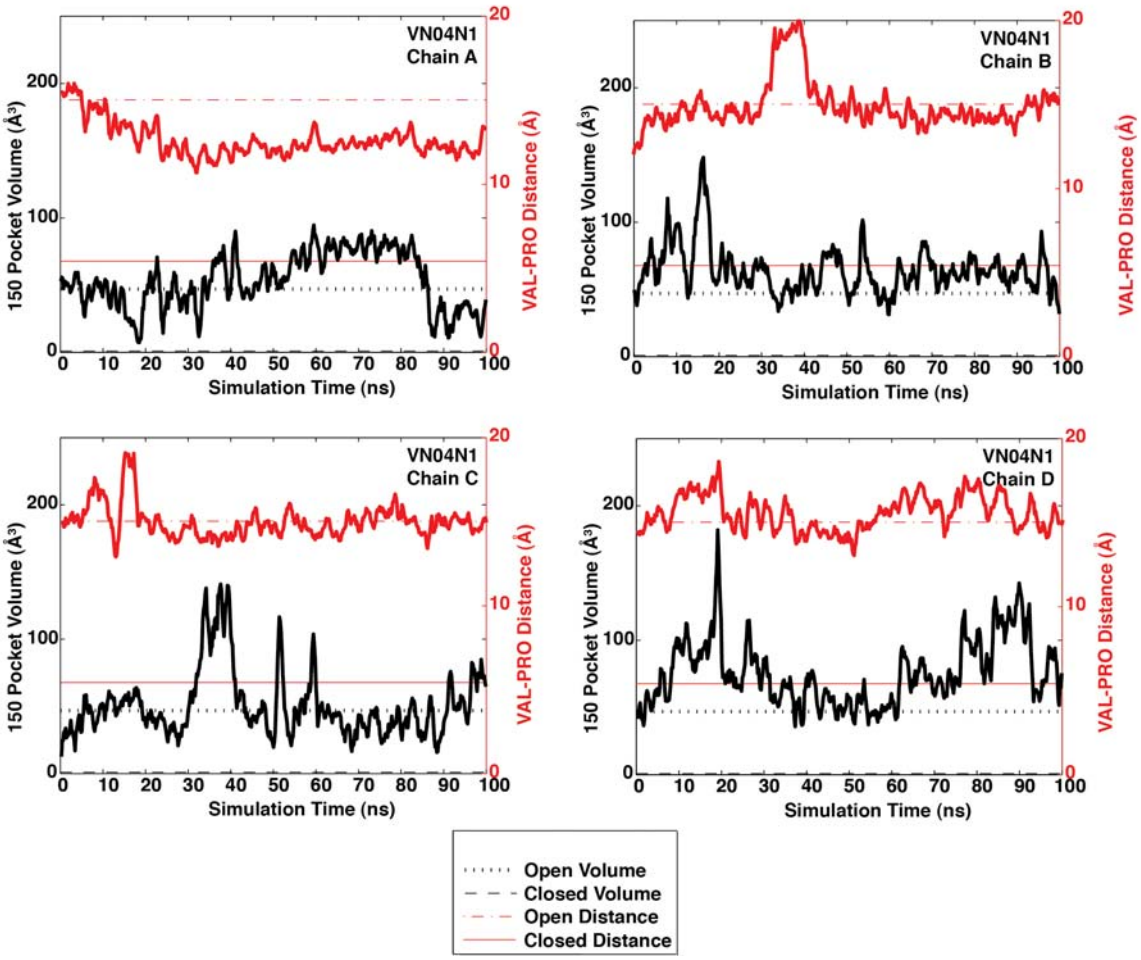

Supplementary Figure S6: Time series analysis of 150-cavity volume and width for VN04N1 system. The distance between alpha carbon of residue 431 (Pro431 in VN04N1) and the closest sidechain carbon of residue 149 (Val149 in VN04N1) is computed and shown in red and the right-side y-axis. On the left side y-axis, the volume of the 150-cavity is computed over the course of simulation. Each plot represents a chain of the neuraminidase tetramer (A-D).

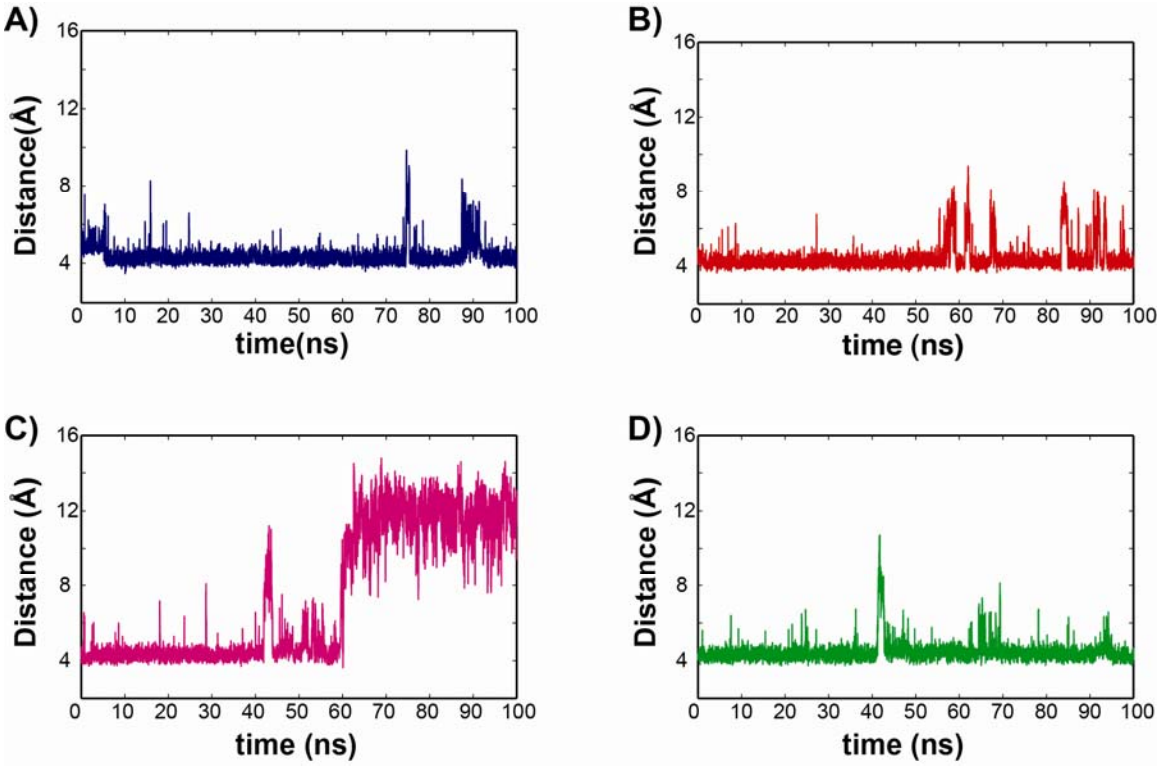

Supplementary Figure S7: Time series plots the key salt bridge that controls 150-cavity formation in the neuraminidase enzymes. The heavy atom distance between residues Asp147 and His150 is shown for all monomers (chains A-D) of the N2 simulation. In Chain C, the salt bridge breaks and does not reform after 60 ns.

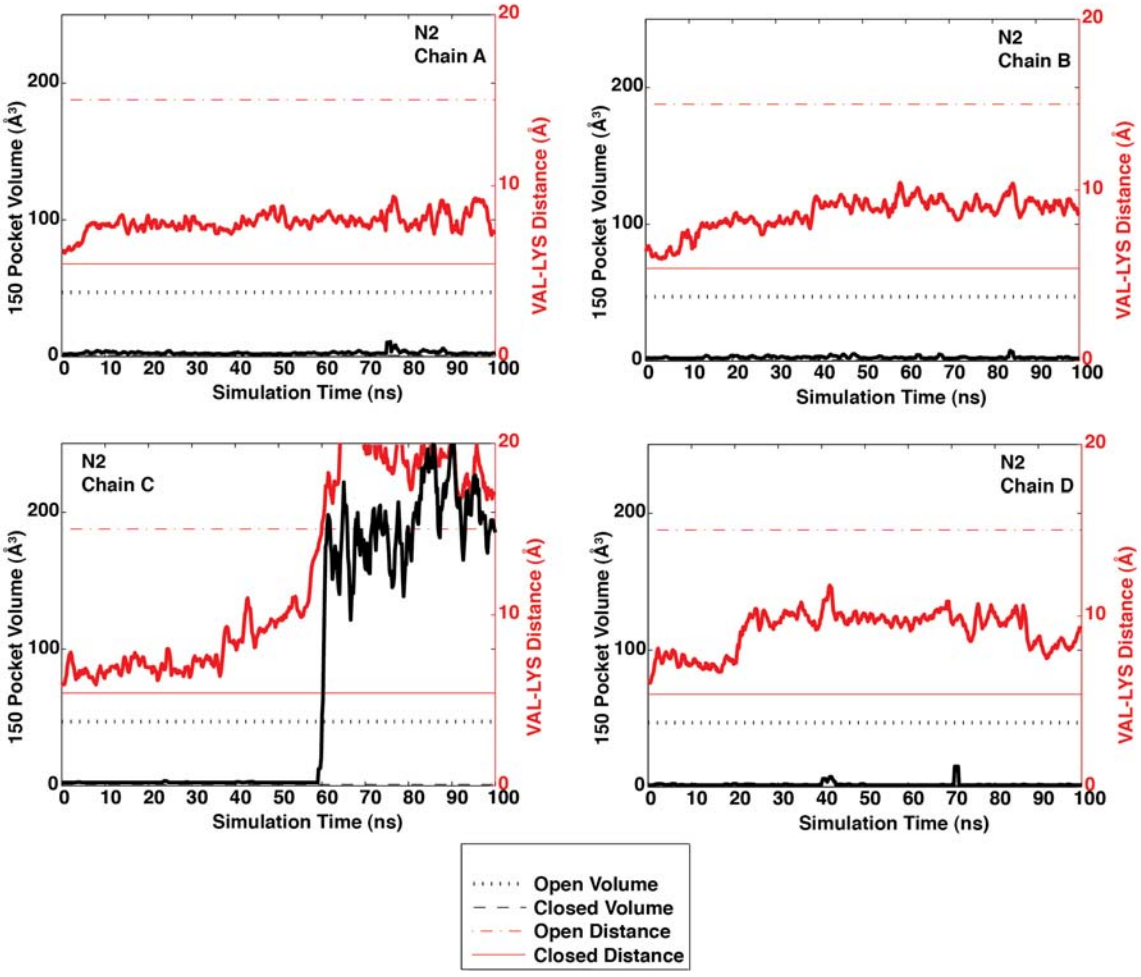

Supplementary Figure S8: Time series analysis of 150-cavity volume and width for N2 system. The distance between alpha carbon of residue 431 (Lys431 in N2) and the closest sidechain carbon of residue 149 (Val149 in N2) is computed and shown in red and the right-side y-axis. On the left side y-axis, the volume of the 150-cavity is computed over the course of simulation. Each plot represents a chain of the neuraminidase tetramer (A-D).

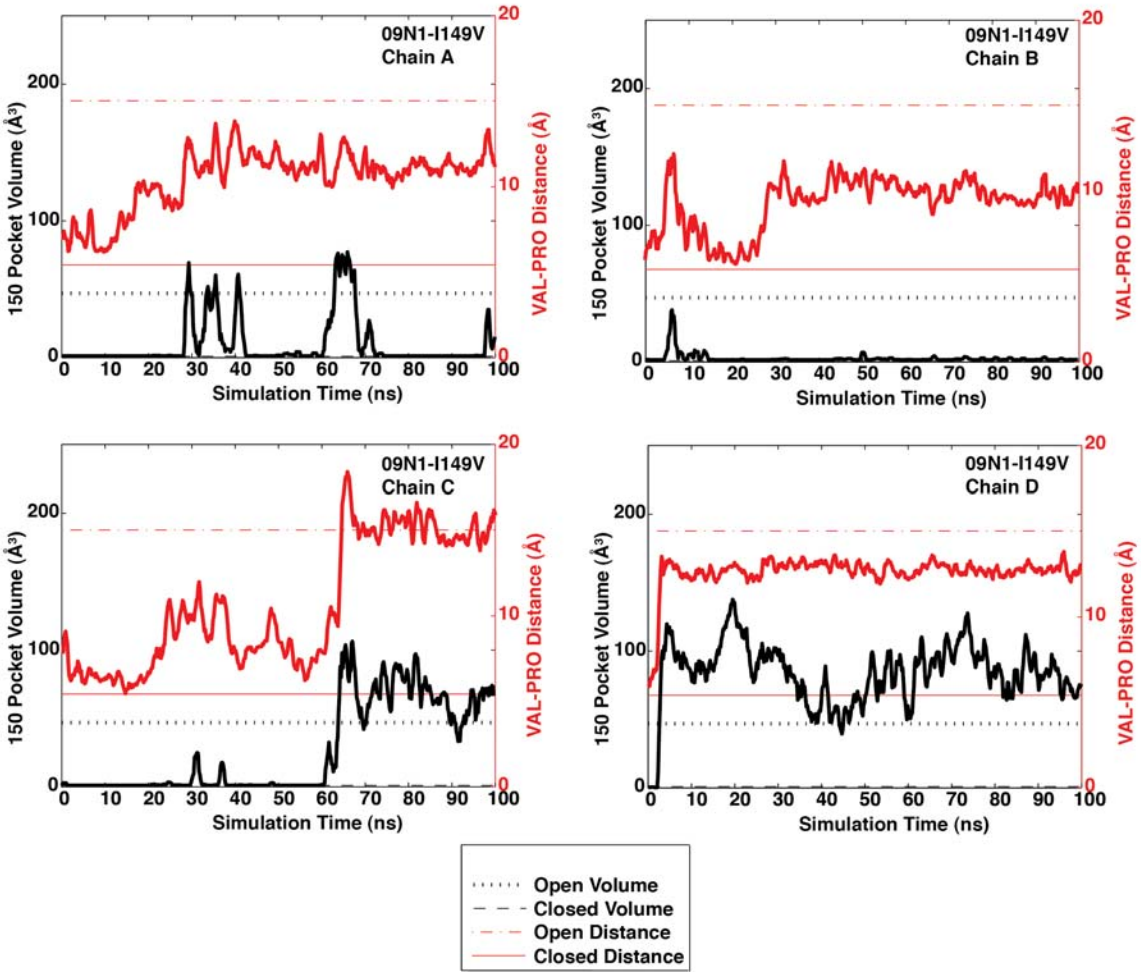

Supplementary Figure S9: Time series analysis of 150-cavity volume and width for 09N1_I149V system. The distance between alpha carbon of residue 431 (Pro431 in 09N1_I149V) and the closest sidechain carbon of residue 149 (Val149 in 09N1_I149V) is computed and shown in red and the right-side y-axis. On the left side y-axis, the volume of the 150-cavity is computed over the course of simulation. Each plot represents a chain of the neuraminidase tetramer (A-D).

Supplementary Tables:

system name	crystal structure	strain	Initial 150-loop state	simulation time (ns)	no. of atoms
N2	1nn2	A/Tokyo/3/67	Closed	100	151,895
09N1	3nss	A/California/04/2009	Closed	100	165,171
09N1_I149V	3nss*	A/California/mutant*	Closed	100	156,338
VN04N1	2hty	A/Vietnam/1203/04	Open	100	112,311

Supplementary Table S1: Description of simulated systems. System name, crystal structure PDB identifier, human strain isolate description, colloquial system description, total simulation time for tetramer simulation, and total number of atoms are shown for each system.

system	cluster 1	cluster 2	cluster 3	no. of clusters
N2	58.8% (closed)	16.7% (closed)	6.8% (open)	24
VN04N1	68.9% (open)	19.4% (open)	11.6% (open)	14
09N1	33.4% (closed)	22.4% (open)	13.7% (open)	25
09N1_I149V	46.9% (closed)	24.8% (open)	15.2% (closed)	14

Supplementary Table S2: RMSD-based clustering results. System name, percent population in the three most dominant clusters and open or closed 150-cavity designation, and the total number of clusters are shown.

Supplementary Table S3: 150-cavity volume for all NA crystal structures (with hydrogen atoms added) and the 3 most dominant cluster structures from the simulations. Structures and volumes correspond to Figure 1 in the main text.

System	Volume (Å^3)	Open/Closed characterization
N2 – crystal structure	0	Closed
N2 MD cluster 1	0	Closed
N2 MD cluster 2	0	Closed
N2 MD cluster 3	284	Open
VN04N1 – crystal structure	36	Open
VN04N1 MD cluster 1	53	Open
VN04N1 MD cluster 2	136	Open
VN04N1 MD cluster 3	65	Open
09N1 crystal structure	0	Closed
09N1 MD cluster 1	0	Closed
09N1 MD cluster 2	77	Open
09N1 MD cluster 3	143	Open
09N1_I149V minimized	0	Closed
09N1_I149V MD Cluster 1	0	Closed
09N1_I149V MD Cluster 2	146	Open
09N1_I149V MD Cluster 2	1	Closed